

Bis[bis(*N*-2-hydroxyethyl,*N*-isopropyl-dithiocarbamato)mercury(II)]₂: crystal structure and Hirshfeld surface analysis

Mukesh M. Jotani^{*I}, Yee Seng Tan^{II} and Edward R. T. Tiekink^{*II}

I Bhavan's Sheth R. A. College of Science, Department of Physics, Ahmedabad, Gujarat 380001, India

II Sunway University, Centre for Crystalline Materials, Faculty of Science and Technology, 47500 Bandar Sunway, Selangor Darul Ehsan, Malaysia

Received; accepted

Keywords: Mercury dithiocarbamate / hydrogen bonding / Hirshfeld surface / crystal structure analysis / X-ray diffraction

Abstract. The presence of both κ^2 -chelating and μ_2, κ^2 -tridentate bridging dithiocarbamate ligands in centrosymmetric $\{\text{Hg}[\text{S}_2\text{CN}(\text{iPr})\text{CH}_2\text{CH}_2\text{OH}]_2\}_2$ (**1**) leads to globular aggregates that are linked into a three-dimensional architecture via hydroxyl-O–H \cdots O(hydroxy) hydrogen bonding. The structure contrasts that of $\text{Hg}[\text{S}_2\text{CN}(\text{CH}_2\text{CH}_2\text{OH})_2]_2$ (**2**; this is a literature structure) in which square planar units are connected into supramolecular chains via Hg \cdots S secondary bonding; chains are connected in the crystal structure by hydroxyl-O–H \cdots O(hydroxy) hydrogen bonding. A Hirshfeld surface analysis on **1** and **2** reveal the influence of O–H \cdots O and Hg \cdots S interactions on the molecular packing as well as the distinctive interactions, such as C–H \cdots S interactions in **1** and C–H \cdots π (HgS₂C) contacts in **2**. A bibliographic survey shows the different structural motifs observed for **1** and **2** are complimented by an additional five motifs for binary mercury(II) dithiocarbamates revealing a fascinating structural diversity for this class of compound.

* Correspondence authors: mmjotani@rediffmail.com (M.M.J.); edwardt@sunway.edu.my (E.R.T.T.)

Introduction

The binary mercury(II) dithiocarbamates, $\text{Hg}[\text{S}_2\text{CNRR}']_2$, are well-known to adopt quite distinct molecular structures in the solid-state [1, 2]. When R, R' = alkyl, these are usually zero-dimensional, being mono- or bi- or even tri-nuclear, depending on the presence of bridging ligands. By contrast, when R, R' = H, a two-dimensional framework is observed [3]; see below for further discussion on this structural diversity. By contrast to the binary mercury(II) dithiocarbamates, cadmium(II) counterparts are usually binuclear owing to the presence of two κ^2 -chelating and two μ_2, κ^2 -tridentate bridging dithiocarbamate ligands leading to five-coordinate coordinate geometries; see [4] for a summary of $\text{Cd}[\text{S}_2\text{CNRR}']_2$

Author	Title	File Name	Date	Page
Mukesh M. Jotani, Yee Seng Tan and Edward R. T. Tiekink	Bis- $[\mu$ - <i>N</i> -2-hydroxyethyl, <i>N</i> -isopropyl-dithiocarbamato]-1:2 $\kappa^3\text{S},\text{S}';\text{S}';2:1\kappa^3\text{S},\text{S}':\text{S}'$]-bis{[<i>N</i> -2-hydroxyethyl, <i>N</i> -isopropyl-dithiocarbamato- $\kappa^2\text{S},\text{S}'$]mercury(II)}: crystal structure and Hirshfeld surface analysis	Hg.docx	30.10.2017	1 (21)

structures. However, the situation with $\text{Cd}[\text{S}_2\text{CNRR}]_2$ changed recently with the discovery of some interesting crystal chemistry with hydroxyethyl-functionalized dithiocarbamate ligands, revealing interchangeable (solvent-mediated) supramolecular isomers and well as a range of co-crystals/decomposition products from relatively standard crystallisation conditions [5]. In first crystallised $\{\text{Cd}[\text{S}_2\text{CN}(\text{iPr})\text{CH}_2\text{CH}_2\text{OH}]_2\}_n$, as a result of equal numbers of μ_2, κ^2 -tridentate bridging dithiocarbamate ligands, a linear coordination polymer was found with hexa-coordinate cadmium centres in addition to the conventional binuclear $\{\text{Cd}[\text{S}_2\text{CN}(\text{iPr})\text{CH}_2\text{CH}_2\text{OH}]_2\}_2$, thermodynamically favoured, form [4, 5]. The polymeric form mimics the recently reported structure of $[\text{Cd}(\text{S}_2\text{NMe}_2)_2]_n$ [6] as well as those of $\{\text{Cd}[\text{S}_2\text{N}(\text{H})\text{R}]_2\}_n$, $\text{R} = n\text{-C}_5\text{H}_{11}$ and $n\text{-C}_{12}\text{H}_{25}$ [7], for which no bi-nuclear species have been reported.

As an extension of studies of the zinc-triad elements with dithiocarbamate ligands functionalised with hydroxyethyl groups [4, 5, 8-11], motivated by the diverse crystal chemistry of the aforementioned cadmium examples, and which produce supramolecular architectures based on directional hydrogen bonding, the crystal and molecular structure of the binuclear title compound, $\{\text{Hg}[\text{S}_2\text{CN}(\text{iPr})\text{CH}_2\text{CH}_2\text{OH}]_2\}_2$, **1**, is described. This structure is compared with the structure of the "parent" compound $\text{Hg}[\text{S}_2\text{CN}(\text{CH}_2\text{CH}_2\text{OH})_2]_2$, **2** [9], which is mononuclear, along with related literature data for the binary mercury(II) dithiocarbamates. The crystal structures of both **1** and **2** [9] have also been subjected to a Hirshfeld surface analysis in order to gain more insight into the molecular packing for these hydroxyethyl-substituted dithiocarbamate structures.

While it is not suggested that mercury(II) dithiocarbamates might prove to possess therapeutic applications owing to the notorious toxicity of mercury, it is interesting to note that heavy-element compounds of hydroxyethyl-substituted dithiocarbamates do exhibit promising biological activity against both cancer models, e.g. gold [12], bismuth [13] and zinc [14], and bacteria, e.g. gold [15], copper and silver [16], providing greater impetus for their study.

Experimental

Synthesis and characterisation

The $\text{Na}[\text{S}_2\text{C}(\text{iPr})\text{CH}_2\text{CH}_2\text{OH}]$ salt was prepared following a literature procedure [17]. Two solutions were prepared. The first solution was prepared by dissolving HgCl_2 (Sigma-Aldrich 1.8 mmol, 0.4887 g) in distilled water (50 ml). The second solution was prepared by dissolving $\text{Na}[\text{S}_2\text{C}(\text{iPr})\text{CH}_2\text{CH}_2\text{OH}]$ (3.6 mmol, 0.7246 g) in distilled water (50 ml). The HgCl_2 solution was added to the dithiocarbamate solution dropwise while stirring under ambient conditions. A light-yellow precipitate formed immediately; the mixture was further stirred for 30 mins. The precipitate

Author	Title	File Name	Date	Page
Mukesh M. Jotani, Yee Seng Tan and Edward R. T. Tiekink	Bis- $[\mu\text{-}N\text{-}2\text{-hydroxyethyl}, N\text{-isopropyl-dithiocarbamato}]_2$: $1:2 \kappa^3\text{S}, \text{S}': \text{S}'; 2:1 \kappa^3\text{S}, \text{S}': \text{S}'$ -bis $\{[N\text{-}2\text{-hydroxyethyl}, N\text{-isopropyl-dithiocarbamato-}\kappa^2\text{S}, \text{S}']\text{mercury(II)}\}$: crystal structure and Hirshfeld surface analysis	Hg.docx	30.10.2017	2 (21)

was extracted with CHCl_3 (Merck, 100 ml) and filtered. Yellow blocks formed after 2 days slow evaporation of the filtrate (Yield: 0.7238 g, 72%).

Crystal structure determination

Intensity data for **1** were measured at 100 K on a Bruker SMART APEX-II CCD diffractometer with graphite-monochromatised Mo $K\alpha$ radiation ($\lambda = 0.71073 \text{ \AA}$). Data processing was with APEX2 and SAINT [18] and the absorption correction was conducted with SADABS [19]. Details of unit cell data, X-ray data collection and structure refinement are given in Table 1. The structure was solved by direct methods [20]. Full-matrix least-squares refinement on F^2 with anisotropic displacement parameters for all non-hydrogen atoms was performed with SHELXL-2014/7 [21]. The C-bound H atoms were placed on stereochemical grounds and refined in the riding model approximation with $U_{\text{iso}} = 1.2\text{--}1.5U_{\text{eq}}(\text{carrier atom})$. The O-bound H atom was located from a difference map and refined with $\text{O--H} = 0.84 \pm 0.01 \text{ \AA}$ and $U_{\text{iso}} = 1.5U_{\text{eq}}(\text{O})$. The maximum and minimum residual electron density peaks of 1.23 and 2.16 e \AA^{-3} , respectively, were located 0.62 and 0.81 \AA from the Hg atom. A weighting scheme of the form $w = 1/[\sigma^2(F_o^2) + (0.011P)^2 + 4.412P]$ where $P = (F_o^2 + 2F_c^2)/3$ was employed. The programs WinGX [22], ORTEP-3 for Windows [22] {at the 50% probability level}, PLATON [23] and DIAMOND [24] were also used in the study.

Tab. 1: Crystallographic data and refinement details for **1**.¹

Formula	$\text{C}_{24}\text{H}_{48}\text{Hg}_2\text{N}_4\text{O}_4\text{S}_8$
Formula weight	1114.38
Crystal colour, habit	yellow, prism
Crystal size/mm	0.06 x 0.07 x 0.12
Crystal system	monoclinic
Space group	$P2_1/c$
$a/\text{\AA}$	10.286(2)
$b/\text{\AA}$	21.916(4)
$c/\text{\AA}$	8.3598(17)
$\beta/^\circ$	97.77(3)
$V/\text{\AA}^3$	1867.3(7)
Z/Z'	2/1
$D_c/\text{g cm}^{-3}$	1.982
$F(000)$	1080
$\mu(\text{MoK}\alpha)/\text{mm}^{-1}$	8.694
Measured data	23578
θ range/ $^\circ$	2.0 – 27.5
Unique data	4285
R_{int}	0.049
Observed data ($I \geq 2.0\sigma(I)$)	3478
R , obs. data; all data	0.034; 0.058
a ; b in wghting scheme	0.011; 4.412
R_w , obs. data; all data	0.048; 0.063
Largest difference peak and hole (\AA^{-3})	1.24, -2.16

¹ Supplementary Material: Crystallographic data (excluding structure factors) for the structures reported in this paper have been deposited with the Cambridge Crystallographic Data Centre as supplementary publication no. CCDC-1453546. Copies of available material can be obtained free of charge, on application to CCDC, 12 Union Road, Cambridge CB2 1EZ, UK, (fax: +44-(0)1223-336033 or e-mail: deposit@ccdc.cam.ac.uk). The list of Fo/Fc-data is available from the corresponding author (ERTT) up to one year after the publication has appeared.

Hirshfeld surface analysis

The program *Crystal Explorer* 3.1 [25] was used to generate Hirshfeld surfaces mapped over d_{norm} , d_e , curvedness and electrostatic potential for each of **1** and **2** [9]. The contact distances d_i and d_e from the Hirshfeld surface to the nearest atom inside and outside, respectively, enable the analysis of the intermolecular interactions through the mapping of d_{norm} . The combination of d_e and d_i in the form of two-dimensional fingerprint plots [26] provides a convenient summary of the most prominent intermolecular contacts in the crystal.

Results and discussion

Molecular structure

The molecular structure of **1** is shown in Figure 1 and selected geometric parameters are listed in Table 2. Crystallography shows the molecule to be binuclear and therefore is formally formulated as bis- $[\mu\text{-}N\text{-}2\text{-hydroxyethyl}, N\text{-isopropyl-dithiocarbamato}]\text{-}1:2\kappa^3 S, S': S'; 2:1\kappa^3 S, S': S']\text{-bis}\{[N\text{-}2\text{-hydroxyethyl}, N\text{-isopropyl-dithiocarbamato-}\kappa^2 S, S']\text{mercury(II)}\}$. The molecule is disposed about a centre of inversion and features two distinct coordination modes for the dithiocarbamate ligands. The S1-containing ligand chelates the Hg atom, forming very similar Hg–S bond lengths, Table 2, with the difference between the Hg–S_{long} and Hg–S_{short} distances being ca 0.02 Å. The S1 atom simultaneously bridges the symmetry-related Hg atom, albeit at a considerably longer separation, i.e. Hg–S1ⁱ is 3.1534 (14) Å for $i: 1-x, 1-y, 2-z$. The S3-containing dithiocarbamate ligand is asymmetrically chelating with the difference between the Hg–S3, S4 bond lengths being over 0.5 Å, Table 2. The different modes of coordination of the dithiocarbamate ligands is reflected in systematic variations in the C–S bond lengths which are experimentally equivalent for C1–S1, S2 but, distinct for C7–S3, S4, where the longer C7–S3 bond is associated with the shorter Hg–S3 bond.

Author	Title	File Name	Date	Page
Mukesh M. Jotani, Yee Seng Tan and Edward R. T. Tiekink	Bis- $[\mu\text{-}N\text{-}2\text{-hydroxyethyl}, N\text{-isopropyl-dithiocarbamato}]$ - $1:2\kappa^3 S, S': S'; 2:1\kappa^3 S, S': S']\text{-bis}\{[N\text{-}2\text{-hydroxyethyl}, N\text{-isopropyl-dithiocarbamato-}\kappa^2 S, S']\text{mercury(II)}\}$: crystal structure and Hirshfeld surface analysis	Hg.docx	30.10.2017	4 (21)

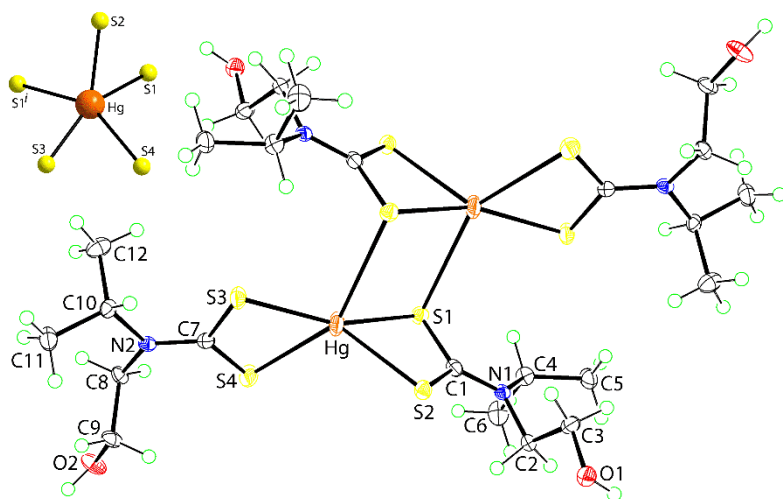


Fig. 1: Molecular structure of **1**. The molecule is disposed about a centre of inversion with unlabelled atoms related by symmetry operation i : 1- x , 1- y , 2- z . Displacement ellipsoids are drawn at the 50% probability level. **The insert highlights the immediate coordination geometry about the mercury atom with S2 lying 2.7360(19) Å above the plane of the remaining four sulphur atoms [r.m.s. deviation = 0.0075 Å].**

Tab. 2: Selected geometric parameters (Å, °) for **1**.[†]

	value		value
Hg–S1	2.5565(12)	Hg–S2	2.5783(12)
Hg–S3	2.3911(13)	Hg–S4	2.9085(14)
Hg–S1 ⁱ	3.1534(14)	C1–S1	1.735(5)
C1–S2	1.730(4)	C7–S3	1.748(5)
C7–S4	1.698(5)	C1–N1	1.327(5)
C7–N2	1.342(5)		
S1–Hg–S2	70.62(4)	S1–Hg–S3	151.44(4)
S1–Hg–S4	102.21(4)	S1–Hg–S1 ⁱ	88.42(4)
S2–Hg–S3	137.93(4)	S2–Hg–S4	118.28(4)
S2–Hg–S1 ⁱ	90.73(4)	S3–Hg–S4	67.64(4)
S3–Hg–S1 ⁱ	90.12(4)	S4–Hg–S1 ⁱ	150.94(3)

[†] Symmetry operation i : 1- x , 1- y , 2- z .

The S₅ coordination geometry defines a distorted square pyramid as quantified by the value of τ , i.e. 0.02, which is very close to the τ value of 0.0 for an ideal square pyramidal geometry cf. 1.0 for an ideal trigonal bipyramid [27]. In this description, the S2 atom occupies the apical position with the r.m.s. deviation for the remaining four sulphur atoms being 0.0075 Å, and with the Hg atom lying 0.6104(6) Å above the S₄ plane. Deviations from the ideal geometry are related in part to the acute chelate angles, Table 2.

Molecular packing

Geometric parameters characterising the intermolecular interactions operating in the crystal structure of **1** are collected in Table 3. Each hydroxy group donates one and accepts one hydrogen bond from the other hydroxy group resulting in flattened zigzag supramolecular chains aligned along the *c*-axis, Figure 2a. As each binuclear molecule has four hydroxyl groups, aligned in different directions, the molecules are connected into a three-dimensional architecture, Figure 2b. Within this framework, methyl-C–H···S interactions are also noted, Table 3.

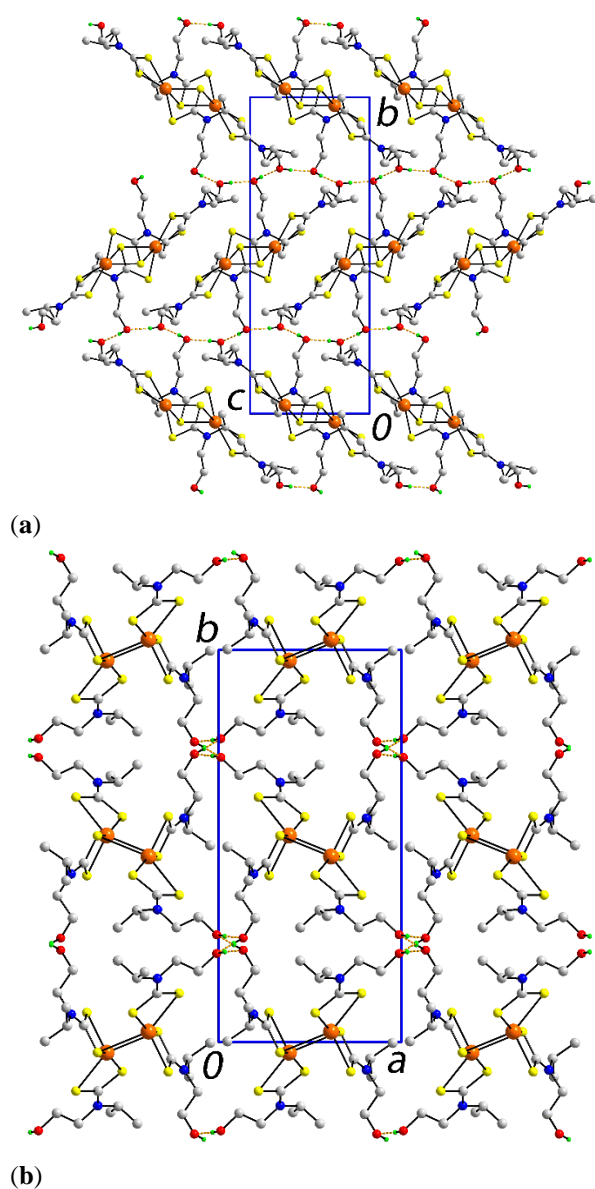


Fig. 2: Two views of the molecular packing in **1** showing the O–H···O hydrogen bonds as orange dashed lines: view in projection down the (a) *a*-axis, and (b) *c*-axis. Non-acidic hydrogen atoms have been omitted for clarity.

In the most closely related structure available for comparison, i.e. Hg[S₂CN(CH₂CH₂OH)₂] [9], **2**, the mercury atom exists within a non-symmetric square planar geometry defined by two asymmetrically coordinating dithiocarbamate

ligands, with Hg–S = 2.4224 (18), 2.907 (3) Å and 2.4158 (19), 2.914 (3) Å. The supramolecular association is based on Hg⋯S secondary interactions [23, 24] and O–H⋯O hydrogen bonding. The former occur above and below the square plane leading to distorted “4+2” octahedral geometries and linear chains of edge-shared octahedra. Within the chains, C–H⋯O and C–H⋯π contacts are also found. Interestingly, the π-system in this case is defined by the HgS₂C chelate ring. Such C–H⋯π(chelate ring) interactions are gaining increasing attention in the supramolecular chemistry of metal 1,1-dithiolates [30-35] and other systems, e.g. acetylacetonates [36]. The chains in **2** are connected into a three-dimensional architecture via O–H⋯O hydrogen bonding; intramolecular O–H⋯O hydrogen bonds also occur.

Author	Title	File Name	Date	Page
Mukesh M. Jotani, Yee Seng Tan and Edward R. T. Tiekink	Bis-[μ- <i>N</i> -2-hydroxyethyl, <i>N</i> -isopropyl-dithiocarbamato]-1:2κ ³ S, <i>S'</i> : <i>S'</i> ;2:1κ ³ S, <i>S'</i> : <i>S'</i>]-bis{[<i>N</i> -2-hydroxyethyl, <i>N</i> -isopropyl-dithiocarbamato-κ ² S, <i>S'</i>]mercury(II)}: crystal structure and Hirshfeld surface analysis	Hg.docx	30.10.2017	7 (21)

Table 3. Summary of intermolecular interactions (A–H···B; Å, °) operating in the crystal structures of **1**.

A	H	B	A–H	H···B	A···B	A–H···B	Symmetry operation
O1	H1o	O2	0.84(4)	1.80(4)	2.630(5)	172(4)	-x, -½+y, 1½-z
O2	H2o	O1	0.84(3)	1.81(3)	2.647(5)	177(7)	-x, 1-y, 1-z
C6	H6b	S2	0.98	2.79	3.597(4)	140	x, y, 1+z
C11	H11a	S1	0.98	2.78	3.425(5)	124	x, y, -1+z

In essence, the molecular packing of **1** may be described as comprising approximately **globular** aggregates of $\{\text{Hg}[\text{S}_2\text{CN}(\text{iPr})\text{CH}_2\text{CH}_2\text{OH}]_2\}_2$ connected by O–H \cdots O hydrogen bonds whereby **2** comprises chains of $\{\text{Hg}[\text{S}_2\text{CN}(\text{CH}_2\text{CH}_2\text{OH})_2]_2\}_n$ connected in the same manner, with both resulting in a three-dimensional architecture. The crystal packing index calculated using PLATON [23] computes to 67.5% for **1** and 73.4% for **2**. This disparity is accounted for by at least two factors. Firstly, the more pronounced secondary Hg \cdots S interactions in **2** cf. **1**. This is allowed by the reduced steric bulk of –CH₂CH₂OH as opposed to –C(H)Me₂, enabling the closer approach of neighbouring molecules in **2**, consistent with literature expectations concerning the influence of steric bulk on supramolecular aggregation patterns for this class of compound [1, 37]. Secondly, the intramolecular O–H \cdots O hydrogen bonding ensures a more compact R/R' region in **2**.

Hirshfeld surface analysis

In order to gain a deeper understanding of the supramolecular association operating in the molecular packing of each of **1** and **2**, especially relating to the distinctive Hg \cdots S secondary interactions and O–H \cdots O hydrogen bonding, an analysis of their Hirshfeld surfaces was conducted. For ease of comparison with square planar **2**, the asymmetric unit of **1**, namely a single Hg[S₂CN(iPr)CH₂CH₂OH]₂ entity, forms the focus of discussion.

The Hirshfeld surfaces generated around the mononuclear motif of **1** having a distorted tetrahedral S₄ coordination geometry, have an overall shape of two fused, orthogonal “buns” **Figures 3a and b** owing to the mutual orthogonal orientation of hydroxyethyl and isopropyl groups on either side of the molecule. This contrasts the **elongated roll** shape for **2**, **Figures 3c and d**. The light-red spots near atoms H6b, H11a, S1 and S2 in **Figure 3b** confirm the involvement of these atoms in the intermolecular C–H \cdots S interactions. Further, a very light-red spot near the S3 atom in **Figure 3b** also indicates the influence of a short interatomic S \cdots S contact in the molecular packing, as quantified in Table 4. The faint red-spots at the quaternary-C6 and methyl-H7A atoms in **Figures 3c and d** indicate the short interatomic contact between them, Table 4. Finally, the presence of intermolecular C–H \cdots O interactions in **2** are evident through the appearance of light-red spots near the corresponding donor and acceptor atoms in **Figure 3d**. The most prominent features of the Hirshfeld surfaces clearly relate to the donors and acceptors corresponding to potential O–H \cdots O hydrogen bonds which appear as bright-red spots, **Figure 3**.

The mapping of the Hirshfeld surfaces over d_{norm} was further evaluated in the –0.35 to 1.3 a.u. range in order to gain greater insight into the molecular packing by enabling the identification of other intermolecular contacts. Thus, the appearance of red spots near the Hg and S1 atoms when d_{norm}

Author	Title	File Name	Date	Page
Mukesh M. Jotani, Yee Seng Tan and Edward R. T. Tiepink	Bis- $[\mu$ - <i>N</i> -2-hydroxyethyl, <i>N</i> -isopropyl-dithiocarbamato]-1:2 κ^3 S,S',S';2:1 κ^3 S,S',S']-bis{[<i>N</i> -2-hydroxyethyl, <i>N</i> -isopropyl-dithiocarbamato- κ^3 S,S']mercury(II)}: crystal structure and Hirshfeld surface analysis	Hg.docx	30.10.2017	9 (21)

was mapped on the Hirshfeld surface of **1** indicate the formation of bridges between the S1 atom and the symmetry related Hg atom, and vice versa, through secondary Hg \cdots S interactions, **Figure 4a**. Bridge formation through two secondary Hg \cdots S interactions between the symmetry related mercury and sulphur atoms in the structure of **2** lead to a distorted “4 + 2” octahedral geometry as indicated by the light-red spots in **Figure 4b**.

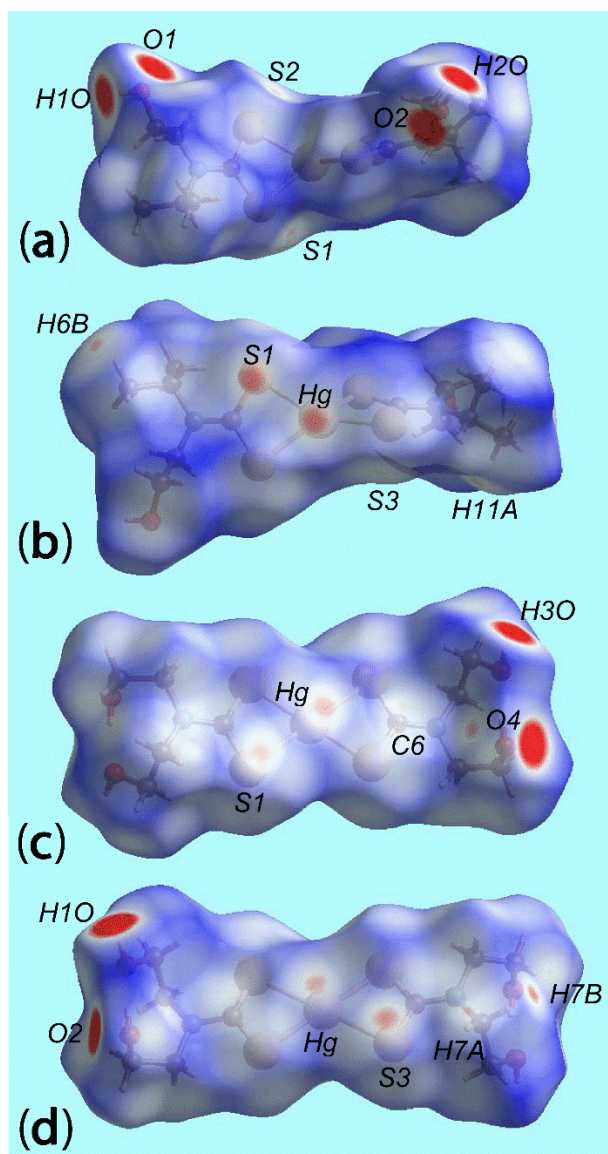


Fig. 3: Views of the Hirshfeld surfaces for (a) and (b) **1**, and (c) and (d) **2**, mapped over d_{norm} highlighting the involvement of atoms in the intermolecular interactions.

Tab. 4: Additional short contacts (Å) in **1** and **2**.

Molecule	Contact	Distance (Å)	Symmetry operation
1	S3··S3	3.577(2)	1-x, 1-y, 2-z
2	C6··H7a	2.74	x, -1+y, z
	O2··H5a	2.60	x, 1+y, z
	H2o··H3o	2.03	1-x, 1-y, -1/2+z
	C5··H3o	2.70	1-x, 1-y, -1/2+z

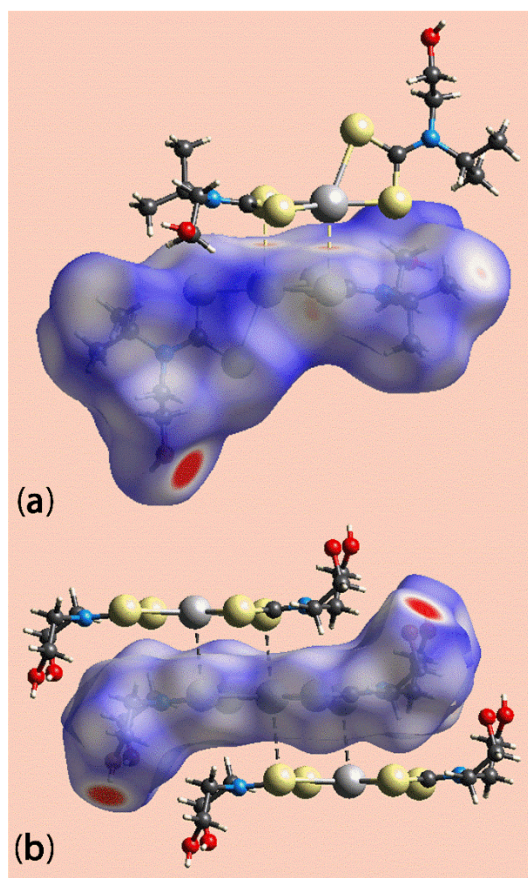


Fig. 4: Views of the Hirshfeld surfaces mapped over d_{norm} , highlighting the regions involved in intermolecular Hg··S secondary bonding interactions: (a) **1** and (b) **2**.

The overall two-dimensional fingerprint (FP) plots for **1** and **2** are shown in **Figure 5a** and those delineated into H··H, O··H/H··O, S··H/H··S, Hg··S/S··Hg and S··S contacts are illustrated in **Figures 5b-f**, respectively; their relative contributions to the overall surfaces are quantified in Table 5.

The FP plots corresponding to H··H contacts for **1** have the largest contribution to the Hirshfeld surface, i.e. 49.4%, and are represented by the points scattered asymmetrically in the middle region and manifested as two pairs of short peaks at $d_e + d_i \sim 2.3$ Å and 2.4 Å, highlighting the dominance of

dispersive forces in the crystal structure. The corresponding FP plot for **2** shows a nearly symmetric (mirror) distribution of points reflected as a saw-tooth with the tips at $d_e + d_i \sim 2.0$ Å, which corresponds to the short interatomic H2o \cdots H3o contact, Table 4. The decrease in the contribution of H \cdots H contacts (40.8%) to the Hirshfeld surface of **2** is due to the reduced hydrogen atom content in **2** cf. **1**, and the involvement of the methylene-H in intermolecular C–H \cdots O and C–H \cdots π (HgS₂C) interactions.

Tab. 5: Percentage contributions of various intermolecular contacts to the Hirshfeld surface areas of **1** and **2**.

Contact	% contribution	
	1	2
H \cdots H	49.4	40.8
O \cdots H/H \cdots O	9.2	14.4
S \cdots H/H \cdots S	29.5	25.9
C \cdots H/H \cdots C	2.7	3.1
Hg \cdots H/H \cdots Hg	3.0	1.9
S \cdots S	1.3	4.4
Hg \cdots S/S \cdots Hg	2.8	4.7
N \cdots H/H \cdots N	0.2	0.8
S \cdots O/O \cdots S	0.3	0.2
S \cdots N/N \cdots S	0.4	0.7
C \cdots S/S \cdots C	0.3	1.7
Hg \cdots C/C \cdots Hg	0.9	1.4

The intermolecular O–H \cdots O hydrogen bonds in both **1** and **2** are indicated by the pair of long spikes in the FP plots delineated into O \cdots H/H \cdots O contacts, Figure 5c, at $d_e + d_i \sim 1.75$ Å and 1.85 Å, respectively. The O \cdots H/H \cdots O contacts in **2** make a greater contribution, i.e. 14.4%, cf. 9.2% in **1**, due to the presence of additional intermolecular C–H \cdots O interactions in **2**.

The asymmetric distribution of points in the FP plots corresponding to S \cdots H/H \cdots S contacts for **1**, Figure 5d, is the result of the non-symmetric tetrahedral coordination geometry and the formation of intermolecular C–H \cdots S interactions showing peaks at $d_e + d_i \sim 2.75$ Å. The pair of peaks at $d_e + d_i \sim 3.1$ Å for **2**, Figure 5d, indicates the influence of the C–H \cdots π (chelate) interactions (see below). By contrast to that for **1**, the FP plot **2** is nearly symmetric in the (d_e , d_i) region between 0.7 and 2.6 Å.

The presence of intermolecular Hg \cdots S interactions in both structures are evident from the FP plots delineated into Hg \cdots S/S \cdots Hg contacts, Figure 5e, being manifested by pairs of short spikes at $d_e + d_i \sim 3.15$ and 3.20 Å, respectively. A single peak at $d_e + d_i \sim 3.6$ Å in the FP plot corresponding to S \cdots S contacts represents the influence of the short interatomic S3 \cdots S3 contact in **1**, Figure 5f and Table 4.

Author	Title	File Name	Date	Page
Mukesh M. Jotani, Yee Seng Tan and Edward R. T. Tiepink	Bis-[μ - <i>N</i> -2-hydroxyethyl, <i>N</i> -isopropyl-dithiocarbamato]-1:2 κ^3 S,S',S':S';2:1 κ^3 S,S':S']-bis{[<i>N</i> -2-hydroxyethyl, <i>N</i> -isopropyl-dithiocarbamato- κ^3 S,S']mercury(II)}: crystal structure and Hirshfeld surface analysis	Hg.docx	30.10.2017	12 (21)

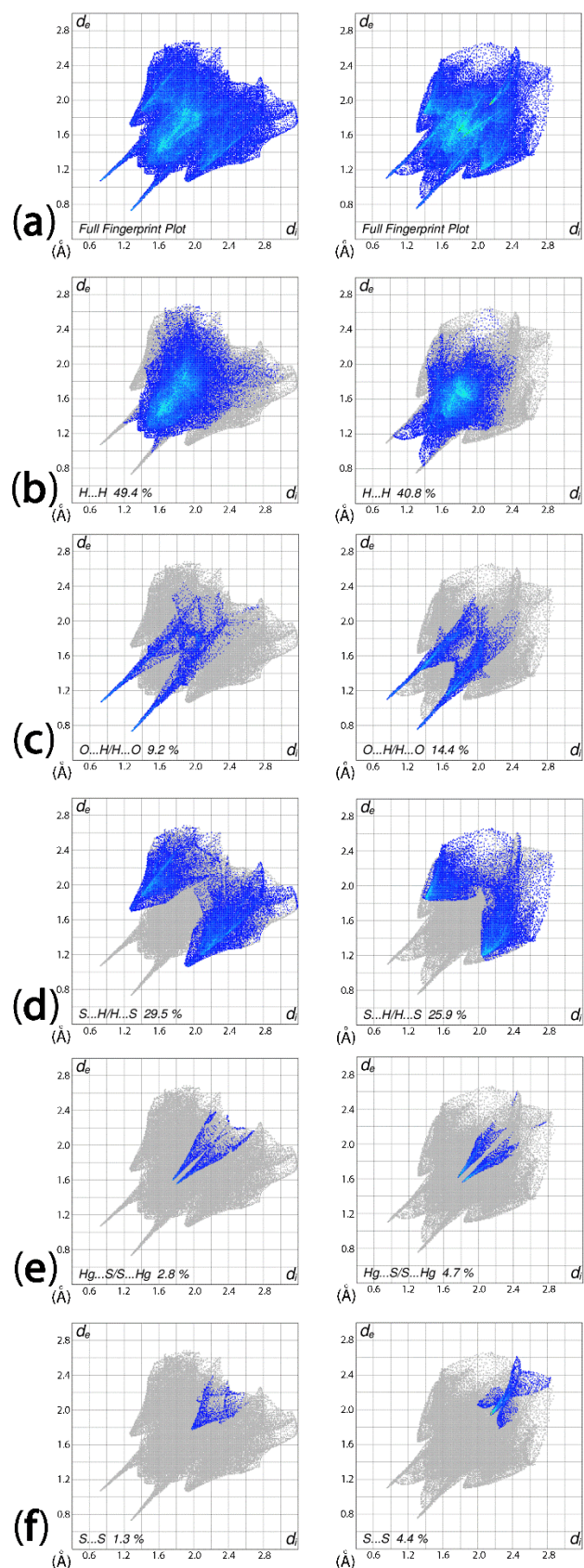


Fig. 5: Fingerprint plots calculated for **1** (left-column) and **2**: (a) overall plots, and plots delineated into (b) H...H, (c) O...H/H...O, (d) S...H/H...S, (e) Hg...S/S...Hg, and (f) S...S contacts.

The presence of $\pi \cdots \pi$ stacking interactions between the symmetry related chelate rings in **2**, Cg \cdots Cg distance = 3.728(3) Å, which complement the Hg \cdots S secondary interactions, is observed from the FP plot with the tips at $d_e + d_i \sim 3.8$ Å, **Figure 5a**. The presence of these $\pi \cdots \pi$ interactions is also indicated through the appearance of a flat region around the chelate ring on the surface mapped with curvedness, **Figure 6**, as well as by the red and blue triangles on the back view of shape-index surface identified with arrows on one of the rings, **Figure 7a**. As identified with arrows on the shape-indexed Hirshfeld surface in **Figure 7b**, the presence of large red spots on the front-side of chelate rings and blue spots near the methylene-C atoms confirm the contribution from C–H \cdots π (chelate) interactions in **2**; analogous $\pi \cdots \pi$ and C–H \cdots π interactions are absent in **1**.

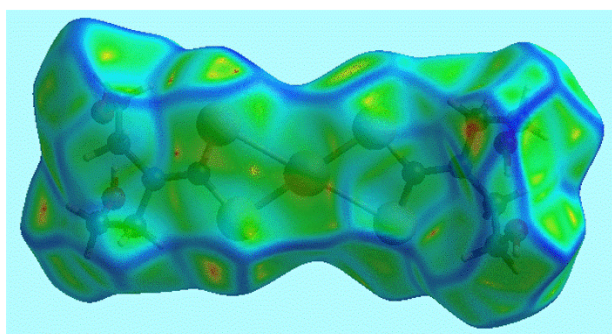


Fig. 6: Hirshfeld surface for **2** mapped with curvedness.

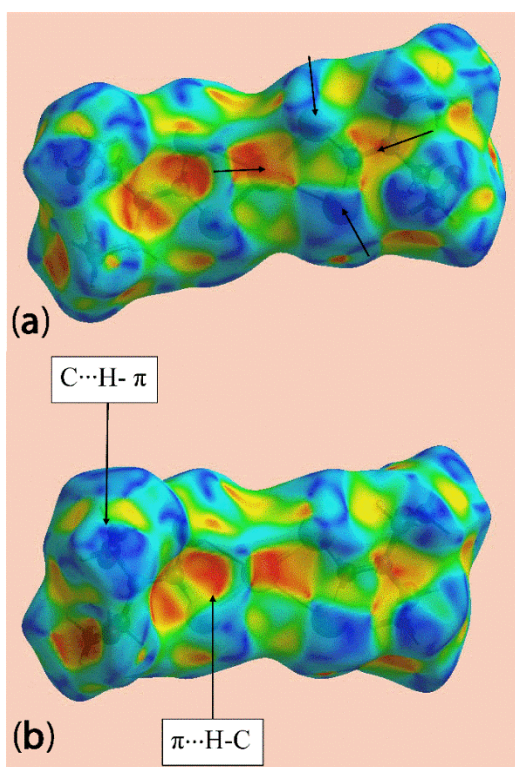


Fig. 7: Hirshfeld surface for **2** mapped with shape-index. The arrows indicate the presence of C–H \cdots π (HgS₂C) contacts.

The final analysis of the molecular packing relates to a relatively new concept, namely, the enrichment ratio (ER) which is also based on Hirshfeld surface analysis [38]; the ratios are summarised in Table 6. The ER values for H \cdots H contacts are close to 1.0 in both **1** and **2** in accordance with expectation [38], indicating no specific preference for these to participate in the molecular packing. The greater enrichment ratio for O \cdots H/H \cdots O contacts in **2** cf. **1** arises as the result of the additional C–H \cdots O interactions in the former. The converse observation is apparent for the S \cdots H/H \cdots S contacts. The large ER values for Hg \cdots S/S \cdots Hg contacts strongly support the bridge formation via these secondary interactions in both **1** and **2**, notably the ER value in **2** is greater consistent with two Hg \cdots S interactions per repeat unit.

Tab. 6: Enrichment ratios for of **1** and **2**.

Contact	1	2
H \cdots H	0.96	1.00
O \cdots H/H \cdots O	1.33	1.55
S \cdots H/H \cdots S	1.15	0.97
Hg \cdots S/S \cdots Hg	2.33	2.80
C \cdots H/H \cdots C	0.96	0.78
C \cdots S/S \cdots C	0.43	1.31
S \cdots S	0.68	1.00

Also notable is the ER value of 1.31 for C \cdots S/S \cdots C contacts in **2**, confirming the contribution of C–H \cdots π (chelate) interactions to the molecular packing. Finally, the presence of $\pi\cdots\pi$ stacking interactions between chelate rings in the structure of **2** is also evident from the ER value of 1.0 for S \cdots S contacts as opposed to a low value of 0.68 for **1** where these interactions are absent.

Literature precedents

As alluded to in the Introduction, the binary mercury(II) dithiocarbamates exhibit a rich structural diversity in the solid-state [1, 2]. A search of the Cambridge Structural Database [39] reveals 33 molecules of the general formula Hg(S₂CNRR')₂, R, R' = alkyl, aryl, plus the new structure reported in the current study and a sole example for the R, R' = H compound, Hg(S₂CNH₂)₂, giving 37 different structures owing to the occurrence of supramolecular isomerism for two formulations [3, 9, 40-64]. An analysis of these structures indicates there is significant structural diversity amongst these, as summarised in Table 7 and Figure 8. A total of 17 structures adopt the binuclear motif found in (I), motif a, illustrated in Figure 8a, allowing for differences in bond lengths, angles and conformation. Four structures adopt a zero-dimensional motif, motif b, based on a distorted S₄ tetrahedron with the R/R' groups being generally large, such as cyclohexyl [46], Figure 8b. An intermediate or pseudo-dimeric motif, motif c (Figure 8c), is found in seven

Author	Title	File Name	Date	Page
Mukesh M. Jotani, Yee Seng Tan and Edward R. T. Tiekink	Bis-[μ -N-2-hydroxyethyl,N-isopropyl-dithiocarbamato]-1:2 κ^3 S,S':S':S':2:1 κ^3 S,S':S':S']-bis{[N-2-hydroxyethyl,N-isopropyl-dithiocarbamato- κ^2 S,S']mercury(II)}: crystal structure and Hirshfeld surface analysis	Hg.docx	30.10.2017	15 (21)

structures which has the appearance of motif a, but the secondary Hg...S separations are greater than 3.35 Å, being the sum of the van der Waals (Σ vdW) radii of Hg and S [65], but less than an arbitrary 3.85 Å, i.e. Σ vdW + 0.5 Å; motif b does not have a Hg...S interaction < 3.85 Å. It has been argued that these structures would be dimeric if the steric bulk of the R/R' groups allowed for a closer approach of the molecules [45].

Subsequent studies with a far wider range of R/R' groups, including aryl rings, residues capable of forming hydrogen bonding interactions, ligands derived from cyclic amines, bifunctional dithiocarbamate ligands, etc. has greatly expanded the range of structures seen in the solid-state for this class of compound. Thus, another zero-dimensional aggregate, motif d, has been observed in the tri-nuclear structure with R = R' = tetrahydroquinoline [55], **Figure 8d**. One-dimensional chains are found in seven Hg(S₂CNRR')₂ compounds. Motif e, featuring a linear chain of edge-shared octahedra with successive Hg(S₂CNRR')₂ residues superimposed when viewed down the axis of the chain, is found in four compounds, e.g. R = R' = CH₂CH₂OH [9] and R = CH₂Ph and R' = CH₂C₅H₄N-4 [63], **Figure 8e**. A variation on this theme is seen in three examples where successive Hg(S₂CNRR')₂ residues are not directly superimposed when the chain is viewed down its axis, e.g. R = R' = Me [40], **Figure 8f**. For completeness, one final structure is mentioned, namely that of Hg(S₂CNH₂)₂ [3], which is a two-dimensional network as all dithiocarbamate ligands are bidentate bridging, motif g, **Figure 8g**.

Author	Title	File Name	Date	Page
Mukesh M. Jotani, Yee Seng Tan and Edward R. T. Tiekink	Bis-[μ - <i>N</i> -2-hydroxyethyl, <i>N</i> -isopropyl-dithiocarbamato]-1:2 κ^3 S,S':S';2:1 κ^3 S,S':S']-bis{[<i>N</i> -2-hydroxyethyl, <i>N</i> -isopropyl-dithiocarbamato- κ^3 S,S']mercury(II)}: crystal structure and Hirshfeld surface analysis	Hg.docx	30.10.2017	16 (21)

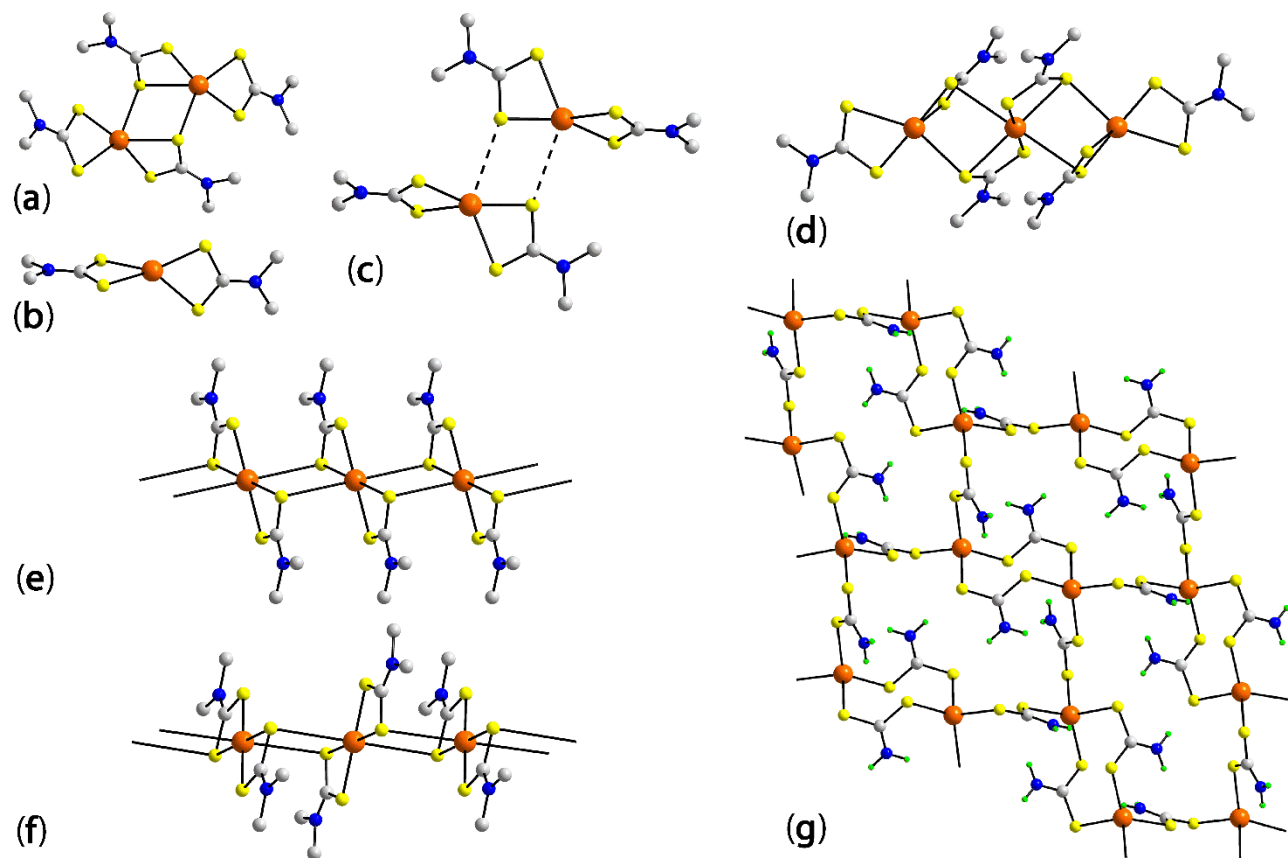


Fig. 8: Zero-, one- and two-dimensional structural motifs observed for $\text{Hg}(\text{S}_2\text{CNRR}')_2$: (a) binuclear, (b) mononuclear, (c) pseudo-binuclear, (d) trinuclear, (e) linear chain, (f) twisted chain, and (g) layer.

Tab. 7: Summary of structural motifs in the crystal structures of binary mercury(II) dithiocarbamates, $\text{Hg}(\text{S}_2\text{CNRR}')_2$.

R	R'	Motif	REFCODE	[Ref.]
Structures with R = R'				
H	H	g	BAWWOL	[3]
Me	Me	f	ROQNEQ	[40]
Et	Et	e	HGETCB01	[41]
Et	Et	a	HGETCB13	[42]
Author	Title	File Name	Date	Page
Mukesh M. Jotani, Yee Seng Tan and Edward R. T. Tiekink	Bis- $[\mu$ - <i>N</i> -2-hydroxyethyl, <i>N</i> -isopropyl-dithiocarbamato]-1:2 κ^3 <i>S,S'</i> : <i>S'</i> ;2:1 κ^3 <i>S,S'</i> : <i>S'</i>]-bis{[<i>N</i> -2-hydroxyethyl, <i>N</i> -isopropyl-dithiocarbamato- κ^2 <i>S,S'</i>]mercury(II)}: crystal structure and Hirshfeld surface analysis	Hg.docx	30.10.2017	17 (21)

Et ^a	Et	a	QIYTOI	[43]
iPr	iPr	b	IPTCHG	[44]
nBu	nBu	a	CAZRAW	[45]
iBu	iBu	c	CAZQID	[45]
Cy	Cy	b	ROPQIW	[46]
CH ₂ CH ₂ OH	CH ₂ CH ₂ OH	e	FOPWAJ	[9]
CH ₂ (2-furyl)	CH ₂ (2-furyl)	a	ROVTED	[47]
CH ₂ Ph	CH ₂ Ph	c	ATADEE	[48]
CH ₂ (3-pyridyl)	CH ₂ (3-pyridyl)	f	YOMYIK	[49]

Structures with R ≠ R'

Me	Ph	a	HAKKIP	[50]
Et	Cy	a	CAZQUP	[45]
iPr	Cy	c	CAZQOJ	[45]
Me	CH ₂ CH ₂ Ph	a	YABJIV	[51]
iPr	CH ₂ CH ₂ OH	a	-	[this work]
Et	Ph	a	YEDQEE	[52]
nBu	R ¹ b	a	XOHBAB	[53]
CH ₂ Ph	CH ₂ (2-furyl)	a	ROVVAB	[47]
CH ₂ CH ₂ Ph	CH ₂ (2-furyl)	a	TUMDOW	[54]
CH ₂ (2-furyl)	CH ₂ CH ₂ (2-(2-thienyl))	a	TULJIV	[54]
CH ₂ Ph	CH ₂ (N-methyl-pyrrol-2-yl)	c	YOMYUW	[49]
CH ₂ (3-pyridyl)	CH ₂ (N-methyl-pyrrol-2-yl)	b	XOBCEY	[55]
CH ₂ (4-pyridyl)	CH ₂ (N-methyl-pyrrol-2-yl)	b	YOMYOQ	[49]
CH ₂ Ph	CH ₂ (3-pyridyl)	e	FODSAU	[56]
CH ₂ Ph	CH ₂ (4-pyridyl)	e	EBUTAY	[57]
CH ₂ Ph	CH ₂ (Fc) ^c	c	MUYXOU	[58]

Structures with R and R' incorporated within a ring

NRR' =				
N(CH ₂) ₄		b	MUWDOX	[59]
N(CH ₂) ₄		a	DUWSIY	[60]
N(CH ₂) ₆		a	VOHKUZ	[61]
4-methylpiperidine		a	KAFFIG	[62]
4-(3-phenylprop-2-en-1-yl)piperazine		c	LIFFEN	[63]
1,2,3,4-dihydroquinoline		a	SODNEG	[64]
1,2,3,4-dihydroquinoline		d	SODNAC	[64]
1,2,3,4-dihydroquinoline ^d		f	SODNIK	[64]

a Isolated as a 1:1 adduct with C₆₀. *b* R¹ is 6-((butyl((sulfanyl)(thioxo)methyl)amino)methyl)dibenzo[b,d]thiophen-4-yl)methyl. *c* Fc is ferrocenyl. *d* Isolated as a 1:1 adduct with 2,2-bipyridyl.

Author	Title	File Name	Date	Page
Mukesh M. Jotani, Yee Seng Tan and Edward R. T. Tiekink	Bis-[μ- <i>N</i> -2-hydroxyethyl, <i>N</i> -isopropyl-dithiocarbamato]-1:2κ ³ S, <i>S</i> : <i>S</i> ';2:1κ ³ S, <i>S</i> : <i>S</i> ']-bis{[<i>N</i> -2-hydroxyethyl, <i>N</i> -isopropyl-dithiocarbamato-κ ² S, <i>S</i> ']mercury(II)}: crystal structure and Hirshfeld surface analysis	Hg.docx	30.10.2017	18 (21)

Conclusions

The binuclear molecule, $\{\text{Hg}[\text{S}_2\text{CN}(\text{iPr})\text{CH}_2\text{CH}_2\text{OH}]_2\}_2$, **1**, is located about a centre of inversion with the Hg–S links between the independent halves arising from the presence of μ_2, κ^2 -tridentate bridging dithiocarbamate ligands. The result is an approximately spherical aggregate. The square pyramidal S_5 donor set in **1** contrasts the square planar, S_4 , geometry in the closely related compound, $\text{Hg}[\text{S}_2\text{CN}(\text{CH}_2\text{CH}_2\text{OH})_2]_2$, **2**. Supramolecular aggregation also occurs in **2** but each mercury atom forms two secondary Hg \cdots S interactions leading to a supramolecular chain. Extensive O–H \cdots O hydrogen bonding occurs in the molecular packing of each compound, linking spheres (**1**) and chains (**2**) into a three-dimensional architecture. Differences in the molecular packing are highlighted in a comparative Hirshfeld surface analysis which reveals the role of the comparatively rare intermolecular C–H \cdots π (HgS₂C) interactions in **2**.

A bibliographic survey of the 37 binary mercury(II) dithiocarbamates now available in the crystallographic literature [39] shows a wide diversity in structures including zero-dimensional, of variable nuclearity, one- and two-dimensional. The subtlety in the structural diversity is reflected in the supramolecular isomers of $\text{Hg}(\text{S}_2\text{CNEt}_2)_2$, i.e. both dimeric [44, 66], motif a, and a linear supramolecular chain [43], motif e, have been reported. Less dramatic are the mono- and bi-nuclear structures i.e. motifs b and a, respectively, found for $\text{Hg}[\text{S}_2\text{CN}(\text{CH}_2)_4]_2$ [61, 62]. Clearly, there is scope for further systematic evaluation of crystallisation for this class of compounds in order to produce an overarching rationalisation for this fascinating crystal chemistry.

Acknowledgments: Sunway University is thanked for support.

References

- [1] E. R. T. Tiekink, *CrystEngComm* **2003**, 5, 101.
- [2] M. J. Cox, Tiekink, E. R. T. *Rev. Inorg. Chem.* **1997**, 17, 1.
- [3] C. Chieh, S. K. Cheung, *Can. J. Chem.* **1981**, 59, 2746.
- [4] Y. S. Tan, S. N. A. Halim, E. R. T. Tiekink, *Z. Kristallogr.* **2016**, 231, 55.
- [5] Y. S. Tan, A. L. Sudlow, K. C. Molloy, Y. Morishima, K. Fujisawa, W. J. Jackson, W. Henderson, S. N. Bt. A. Halim, S. W. Ng, E. R. T. Tiekink, *Cryst. Growth Des.* **2013**, 13, 3046.
- [6] Y. Bing, X. Li, M. Zha, Y. Lu, *Acta Crystallogr. E* **2010**, 66, m1500.
- [7] L. H. van Poppel, T. L. Groy, M. T. Caudle, *Inorg. Chem.* **2004**, 43, 3180.
- [8] R. E. Benson, C. A. Ellis, C. E. Lewis, E. R. T. Tiekink, *CrystEngComm* **2007**, 9, 930.
- [9] R. A. Howie, E. R. T. Tiekink, J. L. Wardell, S. M. S. V. Wardell, *J. Chem. Crystallogr.* **2009**, 39, 293.

Author	Title	File Name	Date	Page
Mukesh M. Jotani, Yee Seng Tan and Edward R. T. Tiekink	Bis- $[\mu$ - <i>N</i> -2-hydroxyethyl, <i>N</i> -isopropyl-dithiocarbamato]-1:2 $\kappa^3\text{S},\text{S}':\text{S}''$;2:1 $\kappa^3\text{S},\text{S}':\text{S}''$]-bis{[<i>N</i> -2-hydroxyethyl, <i>N</i> -isopropyl-dithiocarbamato- $\kappa^2\text{S},\text{S}'$]mercury(II)}: crystal structure and Hirshfeld surface analysis	Hg.docx	30.10.2017	19 (21)

- [10] S. A. M. Safbri, S. N. A. Halim, M. M. Jotani and E. R. T. Tiekink, *Acta Crystallogr. E* **2016**, *72*, 158.
- [11] S. A. M. Safbri, S. N. A. Halim and E. R. T. Tiekink, *Acta Crystallogr. E* **2016**, *72*, 203.
- [12] N. S. Jamaludin, Z.-J. Goh, Y. K. Cheah, K.-P. Ang, J. H. Sim, C. H. Khoo, Z. A. Fairuz, S. N. B. A. Halim, S. W. Ng, H.-L. Seng, E. R. T. Tiekink, *Eur. J. Med. Chem.* **2013**, *67*, 127.
- [13] D. H. A. Ishak, K. K. Ooi, K. P. Ang, A. Md. Akim, Y. K. Cheah, N. Nordin, S. N. B. A. Halim, H.-L. Seng, E. R. T. Tiekink, *J. Inorg. Biochem.* **2014**, *130*, 38.
- [14] Y. S. Tan, K. K. Ooi, K. P. Ang, A. Md Akim, Y.-K. Cheah, S. N. A. Halim, H.-L. Seng and E. R. T. Tiekink, *J. Inorg. Biochem.* **2015**, *150*, 48.
- [15] J.-H. Sim, N. S. Jamaludin, C.-H. Khoo, Y.-K. Cheah, S. N. B. A. Halim, H.-L. Seng, E. R. T. Tiekink, *Gold Bull.* **2014**, *47*, 225.
- [16] N. S. Jamaludin, S. N. B. A. Halim, C.-H. Khoo, B.-J. Chen, T.-H. See, J.-H. Sim, Y.-K. Cheah, H.-L. Seng, E. R. T. Tiekink, *Z. Kristallogr.* **2016** (zkri-16-0003).
- [17] R. A. Howie, G. M. de Lima, D. C. Menezes, J. L. Wardell, S. M. S. V. Wardell, D. J. Young, E. R. T. Tiekink, *CrystEngComm* **2008**, *10*, 1626.
- [18] Bruker. APEX2 and SAINT. Bruker AXS Inc., Madison, Wisconsin, USA, **2009**.
- [19] G. M. Sheldrick, SADABS. University of Göttingen, Germany, **1996**.
- [20] G. M. Sheldrick, *Acta Crystallogr. A* **2008**, *64*, 112.
- [21] G. M. Sheldrick, *Acta Crystallogr. C* **2015**, *71*, 3.
- [22] L. J. Farrugia, *J. Appl. Crystallogr.* **2012**, *45*, 849.
- [23] A. L. Spek, *J. Appl. Crystallogr.* **2003**, *36*, 7.
- [24] K. Brandenburg, DIAMOND. Crystal Impact GbR, Bonn, Germany, **2006**.
- [25] S. K. Wolff, D. J. Grimwood, J. J. McKinnon, M. J. Turner, D. Jayatilaka, M. A. Spackman, Crystal Explorer (Version 3.1), University of Western Australia, **2012**.
- [26] J. J. McKinnon, M. A. Spackman, A. S. Mitchell, *Acta Crystallogr. B* **2004**, *60*, 627.
- [27] A. W. Addison, T. N. Rao, J. Reedijk, J. van Rijn, G. C. Verschoor, *J. Chem. Soc. Dalton Trans.* **1984**, 1349.
- [28] N. W. Alcock, *Adv. Inorg. Chem. Radiochem.* **1972**, *15*, 1.
- [29] I. Haiduc, in *Encyclopedia of Supramolecular Chemistry*, (Eds J. L. Atwood and J. Steed), Marcel Dekker Inc., New York, p. 1215, **2004**.
- [30] D. Chen, C. S. Lai, E. R. T. Tiekink, *Z. Kristallogr.* **2003**, *218*, 747.
- [31] E. R. T. Tiekink, I. Haiduc, *Prog. Inorg. Chem.* **2005**, *54*, 127.
- [32] E. R. T. Tiekink, J. Zukerman-Schpector, *Chem. Commun.* **2011**, *47*, 6623.
- [33] J. Zukerman-Schpector, E. R. T. Tiekink, in *The Importance of Pi-Interactions in Crystal Engineering - Frontiers in Crystal Engineering*, (Eds E. R. T. Tiekink, J. Zukerman-Schpector), John Wiley & Sons Ltd, Singapore, pp. 275-299, **2012**.
- [34] A. N. Gupta, V. Kumar, V. Singh, K. K. Manar, M. G. B. Drew, N. Singh, *CrystEngComm* **2014**, *16*, 9299.
- [35] Y. S. Tan, S. N. A. Halim, K. C. Molloy, A. L. Sudlow, A. Otero-de-la-Roza, E. R. T. Tiekink, *CrystEngComm* **2016**, *18*, 1105.
- [36] M. K. Milčić, V. B. Medaković, D. N. Sredojević, N. O. Juranić, Z. D. Tomić and S. D. Zarić, *Inorg. Chem.* **2006**, *45*, 4755.
- [37] E. R. T. Tiekink, *CrystEngComm* **2006**, *8*, 104.
- [38] C. Jelsch, K. Ejsmont, L. Huder, *IUCrJ* **2014**, *1*, 119.

Author	Title	File Name	Date	Page
Mukesh M. Jotani, Yee Seng Tan and Edward R. T. Tiekink	Bis-[μ - <i>N</i> -2-hydroxyethyl, <i>N</i> -isopropyl-dithiocarbamato]-1:2 κ^3 S,S':S';2:1 κ^3 S,S':S']-bis{[<i>N</i> -2-hydroxyethyl, <i>N</i> -isopropyl-dithiocarbamato- κ^2 S,S']mercury(II)}: crystal structure and Hirshfeld surface analysis	Hg.docx	30.10.2017	20 (21)

- [39] C. R. Groom, I. J. Bruno, M. P. Lightfoot, S. C. Ward, *Acta Crystallogr. B*, **2016**, *72*, 171.
- [40] M. J. Cox, E. R. T. Tiekink, *Z. Kristallogr.* **2010**, *212*, 542.
- [41] P. C. Healy, A. H. White, *J. Chem. Soc., Dalton Trans.* **1973**, 284.
- [42] C. S. Lai, E. R. T. Tiekink, *Z. Kristallogr.- New Cryst. Struct.* **2002**, *217*, 593.
- [43] D. V. Konarev, S. S. Khasanov, D. V. Lopatin, V. V. Rodaev, R. N. Lyubovskaya, *Russ. Chem. Bull.* **2007**, *56*, 2145.
- [44] M. Ito, H. Iwasaki H, *Acta Crystallogr. B* **1979**, *35*, 2720.
- [45] M. J. Cox, E. R. T. Tiekink, *Z. Kristallogr.* **1999**, *214*, 571.
- [46] M. J. Cox, E. R. T. Tiekink, *Main Group Met. Chem.* **2000**, *23*, 793.
- [47] G. Gomathi, S. H. Dar, S. Thirumaran, S. Ciattini, S. Selvanayagam, *C. R. Chim.* **2015**, *18*, 499.
- [48] C. S. Lai, E. R. T. Tiekink, *Appl. Organomet. Chem.* **2004**, *18*, 104.
- [49] M. K. Yadav, G. Rajput, A. N. Gupta, V. Kumar, M. G. B. Drew, N. Singh, *Inorg. Chim. Acta* **2014**, *421*, 210.
- [50] D. C. Onwudiwe, P. A. Ajibade, *Int. J. Mol. Sci.* **2011**, *12*, 1964.
- [51] M. Green, P. Prince, M. Gardener, J. Steed, *Adv. Mater.* **2004**, *16*, 994.
- [52] D. Ondrusova, M. Koman, E. Jona, M. Koman, *Solid State Phenom.* **2003**, *90*, 383.
- [53] E. Guzmán-Percástegui, L. N. Zakharov, J. G. Alvarado-Rodríguez, M. E. Carnes, D. W. Johnson, *Cryst. Growth Des.* **2014**, *14*, 2087.
- [54] S. H. Dar, S. Thirumaran, S. Ciattini, S. Selvanayagam, *Polyhedron* **2015**, *96*, 16.
- [55] G. Rajput, M. K. Yadav, T. S. Thakur, M. G. B. Drew, N. Singh, *Polyhedron* **2014**, *69*, 225.
- [56] V. Singh, V. Kumar, A. N. Gupta, M. G. B. Drew, N. Singh, *New J. Chem.* **2014**, *38*, 3737.
- [57] V. Singh, A. Kumar, R. Prasad, G. Rajput, M. G. B. Drew, N. Singh, *CrystEngComm* **2011**, *13*, 6817.
- [58] A. Kumar, R. Chauhan, K. C. Molloy, G. Kociok-Kohn, L. Bahadur, N. Singh, *Chem.- Eur. J.* **2010**, *16*, 4307
- [59] C. S. Lai, E. R. T. Tiekink, *Appl. Organomet. Chem.* **2003**, *17*, 143.
- [60] M. Altaf, H. Stoeckli-Evans, S. S. Batool, A. A. Isab, S. Ahmad, M. Saleem, S. A. Awan, M. A. Shaheen, *J. Coord. Chem.* **2010**, *63*, 1176.
- [61] A. V. Ivanov, E. V. Korneeva, B. V. Bukvetskii, A. S. Goryan, O. N. Antsutkin, W. Forshling, *Russ. J. Coord. Chem.* **2008**, *34*, 59.
- [62] A. Benedetti, A. C. Fabretti, C. Preti, *J. Crystallogr. Spectrosc. Res.* **1988**, *18*, 685.
- [63] G. Marimuthu, K. Ramalingam, C. Rizzoli, *J. Coord. Chem.* **2013**, *66*, 699.
- [64] N. Srinivasan, S. Thirumaran, S. Ciattini, *RSC Adv.* **2014**, *4*, 22971.
- [65] A. Bondi, *J. Phys. Chem.* **1964**, *68*, 441.
- [66] H. Iwasaki, *Acta Crystallogr. B* **1973**, *29*, 2115.

Author	Title	File Name	Date	Page
Mukesh M. Jotani, Yee Seng Tan and Edward R. T. Tiekink	Bis-[μ - <i>N</i> -2-hydroxyethyl, <i>N</i> -isopropyl-dithiocarbamato]-1:2 κ^3 S,S':S';2:1 κ^3 S,S':S']-bis{[<i>N</i> -2-hydroxyethyl, <i>N</i> -isopropyl-dithiocarbamato- κ^3 S,S']mercury(II)}: crystal structure and Hirshfeld surface analysis	Hg.docx	30.10.2017	21 (21)